Charge Distribution and Atomic Thermal Vibration in Lead Chalcogenide Crystals

By Yasutoshi Noda

Department of Materials Science, Faculty of Engineering, Tohoku University, Aramaki Aoba, Sendai 980, Japan

and Shigeru Ohba,* Shoichi Sato and Yoshihiko Saito*

The Institute for Solid State Physics, The University of Tokyo, Roppongi-7, Minato-ku, Tokyo 106, Japan

Abstract

Charge distribution in crystals of lead chalcogenides, PbX (X = S, Se and Te), has been studied by X-ray diffraction. The structure of PbX is of the rock salt type: cubic, $Fm3m$, a = 5·934 (1), 6·128 (1) and 6·462 (1) Å for PbS, PbSe and PbTe, respectively. Final agreement factors for PbS, PbSe and PbTe were R = 0·015, 0·011 and 0·015 for 144, 147 and 130 independent reflections, respectively. The direct integration of charge density, the observed atomic scattering factors, and the population analysis of the valence electrons unanimously indicated that the Pb atom is negatively charged. This observation suggests predominant covalency for the chemical bond in lead chalcogenide crystals. No overlap density was observed in the deformation density map. The bonding electrons in these crystals may be delocalized like free electrons in metals. The thermal parameters of the Pb atoms were found to be larger than those of the chalcogen atoms and the ratio B_{Pb}/B_X increases in the order: PbS < PbSe < PbTe. Anharmonic thermal vibration of the Pb atom was detected in the difference electron density maps. A positive peak of 2 (0·3) e Å^{-3} was observed in the $\langle 111 \rangle$ direction at 0·4 Å from the Pb nucleus for all three compounds. Its height was reduced to 1 (0·3) e Å^{-3} by introducing anharmonic potential parameters for the Pb atom.

Introduction

Lead chalcogenides are narrow-gap semiconductors. The chemical bond in these crystals has been regarded as ionic, based on the following observations: NaCl-type structure (6:6 coordination); large ionic polarizability (Dalven, 1973); well defined *Reststrahlen* reflectivity bands, that is absorption of far-infrared photons

by the transverse optical phonons (Zemel, 1964; Burnstein, Wheeler & Zemel, 1964; Bylandar & Haas, 1966). On the other hand, they also exhibit covalent character as suggested by small energy gaps, large carrier mobilities, and predominant carrier scattering by acoustical phonons (Ravich, Efimova & Smirnov, 1970). In order to clarify whether the chemical bond in lead chalcogenides is ionic or covalent, the electron density distribution in PbS, PbSe and PbTe crystals was determined by X-ray diffraction.

Experimental

X-ray intensity measurement

Lead chalcogenides were synthesized by the direct reaction of the constituent elements. Lead in ingot form with a nominal purity of 99·9999 wt%, selenium in granular form of purity 99·999 wt%, and tellurium in ingot form of purity 99·9999 wt% were used. Sulfur with a nominal purity of 99·9 wt% was purified by distillation in a vacuum-sealed Pyrex tube. Single crystals were grown by sublimation in controlled chalcogen-vapor pressure (Prior, 1961). The growth temperatures were 1073 K for PbS, 973 K for PbSe and 973 K for PbTe. The vapor-pressure–temperature–composition diagrams indicate that the present growth conditions correspond to the compositions for *p*-type PbS with 1 × 10^{18} holes cm^{-3} (Bloem & Kröger, 1956), for *p*-type PbSe with 1 × 10^{18} holes cm^{-3} (Igaki & Ohashi, 1963), and for *p*-type PbTe with 5 × 10^{18} holes cm^{-3} (Fujimoto & Sato, 1966).

X-ray intensity measurements were carried out on a Rigaku-3 automated four-circle diffractometer using graphite-monochromatized Ag $K\alpha$ radiation. Single crystals, rectangular parallelepipeds with well developed {100} faces of dimensions 0·066 × 0·076 × 0·094, 0·032 × 0·058 × 0·074 and 0·021 × 0·038 × 0·097 mm, were measured for PbS, PbSe and PbTe, respectively. Unit-cell dimensions were determined by a least-squares refinement on the basis of 24 2θ values of

* Present address: Department of Chemistry, Faculty of Science and Technology, Keio University, 3-14-1 Hiyoshi, Kohoku-ku, Yokohama 223, Japan.

Table 1. *Additional crystal data and experimental conditions for X-ray measurement*

	PbS	PbSe	PbTe
Temperature	293 K	295 K	301 K
V (Å³)	208·92 (7)	230·16 (5)	269·79 (4)
D_x (Mg m⁻³)	7·606	8·257	8·242
μ (Ag $K\alpha$) (mm⁻¹)	45·10	49·55	40·18
Elastic constants C_{11}	0·133[a]	0·1237[b]	0·108[c]
(N μm⁻²) $\quad C_{12}$	0·032	0·0193	0·0077
$\quad C_{44}$	0·021	0·0159	0·0134
μr (Ag $K\alpha$) for a sphere with the same volume	2·2	1·6	1·2
X radiation	Ag $K\alpha$	Ag $K\alpha$	Ag $K\alpha$
Monochromator	Graphite	Graphite	Graphite
Collimator	0·3 mm ∅	0·3 mm ∅	0·5 mm ∅
Detector aperture	1·3° (5·5 mm ∅)	1·3 ~ 2·1°	1·3 ~ 2·1°
Scan mode	θ–2θ	θ–2θ	θ–2θ
Scan width (°)	1·4 + 0·5 tan θ	1·3 + tan θ	1·3 + 0·5 tan θ
Scan rate (°min⁻¹ in θ)	0·5 ~ 2·0	0·5 ~ 2·0	0·5 ~ 2·0
$2\theta_{max}$ [(sin $\theta/\lambda)_{max}$]	98° [1·35 Å⁻¹]	104° [1·41 Å⁻¹]	98° [1·35 Å⁻¹]

References: (a) Chudinov (1963a); (b) Lippmann, Kästner & Wanninger (1971); (c) Houston, Strakna & Belson (1968).

reflection 642 and equivalents measured with Ag $K\alpha$ radiation ($\lambda = 0\cdot5608$ Å). Crystal data are listed in the *Abstract* and in Table 1 together with the experimental conditions. All the reflections in a hemisphere of reciprocal space were measured to a 2θ value of about 100° by the θ–2θ scan technique. In all, 2177 non-zero intensities (144 independent) were obtained for PbS, 2198 (147) for PbSe and 1759 (130) for PbTe.

X-ray crystal structure analysis

Corrections for Lorentz and polarization effects were applied. Thermal diffuse scattering (TDS) was corrected by the program *TDS2* (Stevens, 1974) using the elastic-constant data listed in Table 1. Absorption correction was made by the numerical Gauss-integration method (Busing & Levy, 1967). For example, the transmission factor, A, for PbSe was in the range from 0·08 to 0·27. The absorption-correction factor did not change significantly when the number of divisions increased from 8 to 12 in the Gaussian integration.

Parameters were refined by the full-matrix least-squares program *RADIEL* (Coppens, Guru Row, Leung, Stevens, Becker & Yang, 1979) on the basis of all the observed reflections. The function minimized was $R_w(F) = [\sum w(|F_o| - |F_c|)^2/\sum w|F_o|^2]^{1/2}$, where the weight was defined by $w^{-1} = [\sigma_F(\text{counting statistics})]^2 + (0\cdot02|F_o|)^2$. Refinement information is in Table 2. Parameters converged after the following three steps. First, a scale and isotropic thermal parameters were refined. Secondly, an isotropic secondary-extinction parameter was introduced. Finally, the type I anisotropic secondary-extinction correction (Coppens & Hamilton, 1970) was employed. For example, the R

factor $(= \sum ||F_o| - |F_c||/\sum |F_o|)$ for PbSe was 0·073 with no extinction correction, 0·038 with isotropic and 0·031 with anisotropic extinction correction. The smallest extinction factor y $(= F_o^2/F_c^2)$ is 0·5 for 200. Internal agreement factors between equivalent reflections, R_F $(= \sum ||F_o| - \langle|F_o|\rangle|/\sum |F_o|)$, are about 0·03 for all three crystals. After averaging equivalent reflections, the final R value became 0·015 for PbS (144 unique reflections), 0·011 for PbSe (147), and 0·015 for PbTe (130).*

The scattering factors of the neutral atoms as well as the anomalous-scattering factors were taken from *International Tables for X-ray Crystallography* (1974).

Elastic-constant data for PbSe reported by Lippmann, Kästner & Wanninger (1971) differ markedly from those reported by Chudinov (1963b) as listed in Table 3. The disagreement has not been rationalized as Lippmann *et al.* described in their paper. For this particular case, a refinement was also made using the elastic-constant data of Chudinov. Agreement factors with TDS correction using the data of Chudinov and those of Lippmann *et al.* were $R = 0\cdot013$ and 0·011, respectively. For reference, a refinement was also made without TDS correction

---

* Lists of structure factors for the three compounds have been deposited with the British Library Lending Division as Supplementary Publication No. SUP 38323 (7 pp.). Copies may be obtained through The Executive Secretary, International Union of Crystallography, 5 Abbey Square, Chester CH1 2HU, England.

Table 2. *Refinement information*

	PbS	PbSe	PbTe
Observed reflections (n)	2251	2418	1978
$R(F)$	0·035	0·031	0·030
$R_w(F)$	0·040	0·040	0·038
$[\sum w(|F_o| - |F_c|)^2/(n-p)]^{1/2}$	1·08	1·12	1·13
Internal agreement factor between equivalent reflections	0·031	0·029	0·028
Unique reflections	144	147	130
$R(F)$	0·015	0·011	0·015
$R_w(F)$	0·015	0·013	0·016
Thermal parameter (Å²) B_{Pb}	1·283 (3)	1·427 (3)	1·781 (5)
B_X	1·247 (11)	1·130 (4)	1·228 (4)

Table 3. *Thermal parameters of* PbSe *from three refinements of an X-ray study:* (a) *without TDS correction;* (b) *after TDS correction with the elastic-constant data of Chudinov* (1963b); *and* (c) *after TDS correction with the elastic-constant data of Lippmann et al.* (1971)

		(a)	(b)	(c)
Elastic constants (N μm⁻²)	C_{11}		0·4039	0·1237
	C_{12}		0·3189	0·0193
	C_{44}		0·01623	0·0159
Thermal parameters (Å²)	B_{Pb}	1·327 (3)	1·388 (3)	1·427 (3)
	B_{Se}	1·030 (4)	1·092 (4)	1·130 (4)
Agreement factors for 147	$R(F)$	0·014	0·013	0·011
unique reflections	$R_w(F)$	0·016	0·015	0·013

($R = 0.014$). In view of the R factors, the elastic constants obtained by Lippmann *et al.* look better than those by Chudinov. It is noted that the thermal parameters increased by *ca* 9% after the TDS correction.

The integrated intensities of 002 were measured with variation of the angle of rotation, ψ, around the scattering vector, in order to check the absorption correction and to confirm the anisotropic secondary-extinction effect. After the absorption correction, the largest variation of $|F_{002}|$ for PbSe was reduced from 50 to 20%. The isotropic secondary-extinction correction could not reduce the rest of the variation. On the other hand, it decreased to 10% by introducing anisotropy in the secondary-extinction correction and the R value was reduced from 0.038 to 0.031. This shows significant anisotropy in the secondary-extinction effect.

Results and discussion

Effective atomic charge

The expected electronic configurations for the atoms in PbX using an ionic-bond model are Pb^{2+}: $(6s)^2$ and X^{2-}: $(ns)^2(np)^6$ ($n = 3$, 4 or 5 for $X = $ S, Se or Te, respectively). Any covalency leads to a redistribution of charge density, so by measuring the effective atomic charge it should be possible to determine whether the chemical bond in PbX is ionic or covalent. Direct integration of charge density, observed atomic scattering factor and the population analysis of valence orbitals unanimously gave a negative atomic charge to Pb. This indicates that electrons are transferred from the chalcogen to the Pb atom. Thus, the present study would suggest that the interaction has a predominantly covalent character.

The number of electrons in a sphere centered at each atomic nucleus was calculated by the direct-integration method (Sakurai, 1967) with correction for series termination (Kobayashi, Marumo & Saito, 1972). For reference, theoretical values for the free Pb^0 and X^0 atoms were calculated with theoretical scattering factors (*International Tables for X-ray Crystallography*, 1974). The differences between these observed and theoretical values are plotted in Fig. 1 against sphere radius. For example, the number of electrons in the sphere of octahedral radius of Pb (1.66 Å), proposed by Suchet (1965) assuming iono-covalent bonds with p^3 orbitals, was estimated to be 81.0 (5), 81.5 (5) and 81.7 (4) for PbS, PbSe and PbTe, respectively.* That of the free Pb^0 atom is 80.6. The number of electrons observed around the Pb atom is

* The standard deviation assigned to the number of electrons and to the deformation density was derived from the errors in $|F_o|$ and an error in the scale factor (Toriumi & Saito, 1978).

larger than that around the free Pb^0 atom, while around the chalcogen atoms it is less than those around the free X^0 atoms.

Atomic scattering factors for Pb and X atoms are obtained by forming the sum and difference of the observed structure factors which are shown as two curves dependent on whether reflection indices are all-even or all-odd (Brill, 1967). As shown in Fig. 2, the observed scattering factors of the Pb atom exceed the theoretical scattering curve for the free Pb^0 atom, and those of the X atoms are below the theoretical curves for free X^0 atoms in the region $\sin \theta/\lambda < 0.3$ Å^{-1}. This shows that the Pb atom is negatively and the chalcogen atoms are positively charged.

A valence-electron population analysis was also performed. The $6s$ and $6p$ electrons of Pb and ns and np electrons of X spread so diffusely that the scattering factors of these orbitals have significant values only in the very-low-angle region ($\sin \theta/\lambda < 0.3$ Å^{-1}). The same problem occurs for crystals containing alkali-metal atoms. Following Coppens *et al.*(1979), the next inner shell was tentatively included in the valence shell as listed in Table 4. Total charge in the unit cell was kept as neutral, and the κ parameter for expansion or
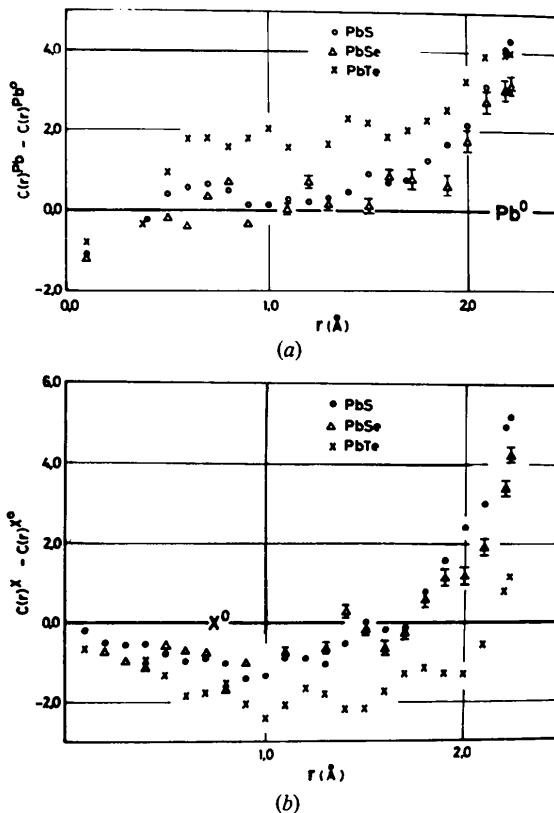

Fig. 1. The difference between numbers of electrons observed in a sphere centered at each atomic nucleus and the theoretical values for the free neutral atoms is plotted against the radius of the sphere for (a) Pb and (b) chalcogen atoms.

contraction of the valence shells was not introduced. The effective charge of Pb was determined to be -1.2 (2), -0.9 (1) and -2.7 (1) for PbS, PbSe and PbTe, respectively. Scattering factors of core and valence electrons for Pb and Te atoms were calculated from the Hartree–Fock wavefunctions of Mann's (1968) table; for S and Se, they were taken from the table given by Fukamachi (1971), which was obtained by the use of the wavefunctions of Clementi (1965) calculated by the Roothaan–Hartree–Fock method.

Residual electron density

Sections of the difference syntheses on the (110) plane for PbS, PbSe and PbTe are presented in Figs. 3(a), 3(b) and 3(c), respectively. They have a standard
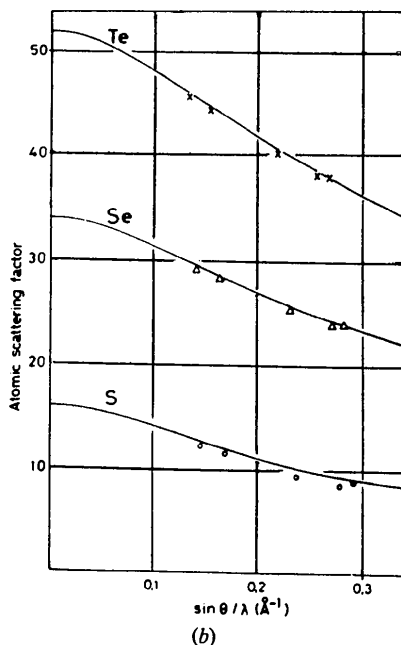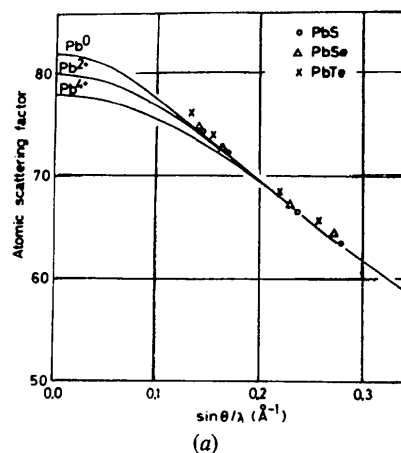
Table 4. *Information regarding valence-electron population analysis*

Valence orbitals

Pb	$(4s,4p,4d,4f)$ + $(5s,5p,5d)$ + $(6s)^2(6p)^2$
S	$(2s,2p)$		+ $(3s)^2(3p)^4$
Se	$(3s,3p,3d)$		+ $(4s)^2(4p)^4$
Te	$(4s,4p,4d)$		+ $(5s)^2(5p)^4$

Effective charge of Pb

PbS	-1.2 (2)
PbSe	-0.9 (1)
PbTe	-2.7 (1)

deviation of 0.1 e Å^{-3} at a general position.* On the Pb—X bond axes no positive peak higher than 0.1 e Å^{-3} is observed, in contrast to the deformation density maps of diamond (Göttlicher & Wölfel, 1959) and silicon (Aldred & Hart, 1973; Yang & Coppens, 1974) which show electron accumulation due to the covalent-bond formation.

For covalency in the PbX crystals, a resonance scheme of p^3 covalent bonds was proposed by Krebs (1957). The electronic configurations for the atoms in this model are Pb$^-$: $(6s)^2(6p)^3$ and X^+: $(ns)^2(np)^3$. The covalent bond is formed between each atom and its six neighbors through incomplete occupancy of six electron-pair bond orbitals by 10 electrons. Such a resonating covalent bond means a metallic bond, which is a matter of definition (Lucovsky & White, 1973; Schiferl, 1974). The reason why no overlap density is observed for PbX crystals may be that the bonding electrons in these crystals are delocalized like free electrons in metals.

Atomic thermal vibration

In Fig. 3, well defined maxima are observed in the ⟨111⟩ directions at about 0.4 Å from the Pb nucleus for all three compounds. The peak height is ca 2 (0.3) e Å^{-3}. This charge asphericity may be attributed to the anharmonic thermal vibration of the Pb atoms, judging from the short distance from the Pb nucleus to the positive peaks and their direction away from the nearest neighbors. With the anharmonic approximation (Willis, 1969), fourth-order potential parameters, γ and δ, for the Pb atoms were introduced in addition to the harmonic parameter α for the Pb and chalcogen atoms. The results of the refinement are listed in Table 5. The parameter α_{Pb} decreases from 2.861 (2) for PbS to 2.270 (2) $\times$ 10^{-19} J Å^{-2} for PbTe, while α_X remains almost constant at $2.6 \pm 0.1 \times 10^{-19}$ J Å^{-2}. The positive δ shows lower potential in the ⟨111⟩ than in the ⟨100⟩ directions. The deformation density map for PbSe obtained after introduction of the anharmonic potential parameters is shown in Fig. 3(d). The positive peaks around the Pb nucleus in the ⟨111⟩ directions were reduced from 2 (0.3) to 1 (0.3) e Å^{-3}.

Fig. 2. Comparison between the observed atomic scattering factors and the theoretical curves for (a) Pb and (b) chalcogen atoms.

* See previous footnote.

This suggests that there might be some anharmonic motion of the Pb atoms.

The thermal parameters of the Pb atoms are generally larger than those of the X atoms as listed in Table 2. The ratios B_{Pb}/B_X are 1·03, 1·26 and 1·45 for X = S, Se and Te, respectively. The analysis of the anharmonic potential parameters indicates that the increase in the ratio is mainly due to the decrease in the harmonic potential parameter of the Pb atoms. The IV–VI ternary chalcogenides, $Pb_{1-x}Ge_xTe$ ($x \geq 0·01$) and $Pb_{1-x}Sn_xTe$ ($x \geq 0·35$) exhibit a phase transformation from high-temperature NaCl-type to a low-temperature As-type structure and the transition temperature increases with alloy composition (Takaoka & Murase, 1979). This lattice instability of the Pb(Ge,Sn)Te crystals has been explained by assuming lattice polarization and softening of the transverse optical phonons (Murase, 1980). Even in pure PbTe crystals, the relatively large displacement of the Pb sublattice to that of the Te sublattice as well as the anharmonic thermal vibration of the Pb atoms along the $\langle 111 \rangle$ directions were observed. These thermal vibrations of the Pb atom are enhanced by the alloying elements Ge or Sn and make a lattice more unstable.

Table 5. *Potential parameters for the* Pb *and chalcogen atoms in the anharmonic approximation*

The parameter α represents harmonic, γ isotropic anharmonic and δ anisotropic anharmonic coefficients of potential.

	α_{Pb} (10^{-19} J Å^{-2})	γ_{Pb} (10^{-19} J Å^{-4})	δ_{Pb} (10^{-19} J Å^{-4})	α_X (10^{-19} J Å^{-2})
PbS	2·861 (2)	−2·17 (2)	0·8 (3)	2·523 (21)
PbSe	2·626 (2)	−2·05 (2)	0·8 (2)	2·769 (8)
PbTe	2·270 (2)	−2·01 (2)	0·2 (2)	2·604 (6)

Calculations were carried out on the FACOM 230-48 and FACOM M-160F computers at the Institute for Solid State Physics, the University of Tokyo.

Fig. 3. Sections of the difference syntheses in the (110) plane for (a) PbS, (b) PbSe and (c) PbTe. Contours are drawn at intervals of 0·5 e Å^{-3}. Negative contours are broken, zero being chain-dotted. (d) The same section for PbSe after the introduction of anharmonic potential parameters.

References

ALDRED, P. J. E. & HART, M. (1973). *Proc. R. Soc. London Ser. A*, **332**, 223–238.
BLOEM, J. & KRÖGER, F. A. (1956). *Z. Phys. Chem. (Frankfurt am Main)*, **7**, 1–14.
BRILL, R. (1967). *Solid State Physics*, Vol. 20, edited by F. SEITZ, D. TURNBULL & H. EHRENREICH, pp. 1–35. New York: Academic Press.
BURNSTEIN, E., WHEELER, R. & ZEMEL, J. (1964). *Physics of Semiconductors, Proceedings of the 7th International Conference*, edited by M. HULIN, pp. 1065–1066. New York: Academic Press.
BUSING, W. R. & LEVY, H. A. (1967). *Acta Cryst.* **22**, 457–464.
BYLANDAR, E. G. & HAAS, M. (1966). *Solid State Commun.* **4**, 51–53.
CHUDINOV, A. A. (1963a). *Fiz. Tverd. Tela (Leningrad)*, **5**, 1458–1460.
CHUDINOV, A. A. (1963b). *Kristallografiya*, **8**, 473–475.
CLEMENTI, E. (1965). *Tables of Atomic Functions. IBM J. Res. Dev.* **9**, supplement.
COPPENS, P., GURU ROW, T. N., LEUNG, P., STEVENS, E. D., BECKER, P. J. & YANG, Y. W. (1979). *Acta Cryst.* A**35**, 63–72.
COPPENS, P. & HAMILTON, W. C. (1970). *Acta Cryst.* A**26**, 71–83.
DALVEN, R. (1973). *Solid State Phys.* **28**, 179–224.
FUJIMOTO, M. & SATO, Y. (1966). *Jpn. J. Appl. Phys.* **5**, 128–133.
FUKAMACHI, T. (1971). *Mean X-ray Scattering Factors Calculated from Analytical Roothaan–Hartree–Fock Wave Functions by Clementi*. Tech. Rep. Ser. B, No. 12, Institute for Solid State Physics, Univ. of Tokyo.
GÖTTLICHER, S. & WÖLFEL, E. (1959). *Z. Elektrochem.* **63**, 891–901.
HOUSTON, B., STRAKNA, R. E. & BELSON, H. S. (1968). *J. Appl. Phys.* **39**, 3913–3916.
IGAKI, K. & OHASHI, N. (1963). *J. Phys. Soc. Jpn*, **18**, Suppl. 2, 143–147.
International Tables for X-ray Crystallography (1974). Vol. IV. Birmingham: Kynoch Press.
KOBAYASHI, A., MARUMO, F. & SAITO, Y. (1972). *Acta Cryst.* B**28**, 2709–2715.
KREBS, K. (1957). *Z. Elektrochem.* **61**, 925–934.
LIPPMANN, G., KÄSTNER, P. & WANNINGER, W. (1971). *Phys. Status Solidi A*, **6**, K159–K161.
LUCOVSKY, G. & WHITE, R. M. (1973). *Phys. Rev. B*, **8**, 660–667.
MANN, J. B. (1968). *Atomic Structure Calculations. II. Hartree–Fock Wave Functions and Radial Expectation Values: Hydrogen to Lawrencium*. Los Alamos Scientific Laboratory, Univ. of California.
MURASE, K. (1980). *J. Phys. Soc. Jpn*, **49**, Suppl. *A*, 725–732.
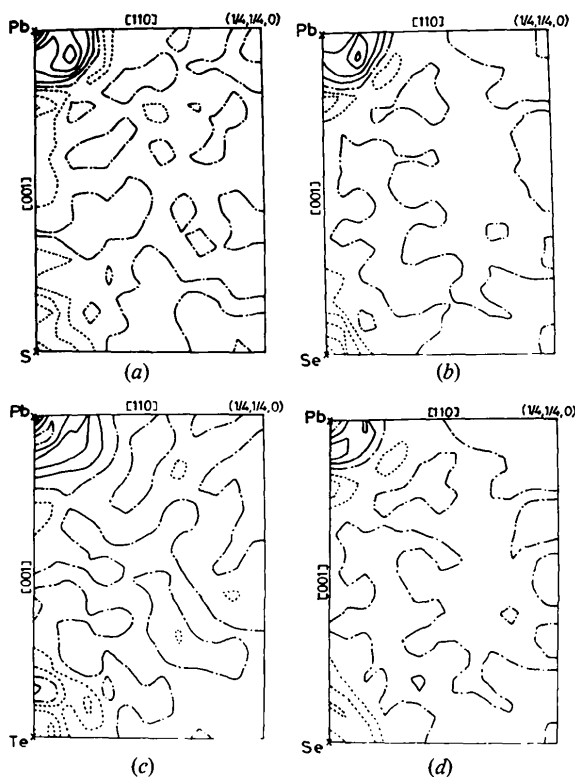PRIOR, A. C. (1961). *J. Electrochem. Soc.* **10**, 82–87.

RAVICH, YU. I., EFIMOVA, B. A. & SMIRNOV, I. A. (1970). *Semiconducting Lead Chalcogenides*, pp. 90–100 (translated by A. TYBULEWICZ). New York: Plenum.

SAKURAI, T. (1967). *X-ray Crystal Structure Analysis*, pp. 218–220. Tokyo: Shokabo.

SCHIFERL, D. (1974). *Phys. Rev. B*, **10**, 3316–3329.

STEVENS, E. D. (1974). *Acta Cryst.* A**30**, 184–189.

SUCHET, J. P. (1965). *Chemical Physics of Semiconductors* (translated by E. HEASELL). London: Van Nostrand.

TAKAOKA, S. & MURASE, K. (1979). *Phys. Rev. B*, **20**, 2823–2833.

TORIUMI, K. & SAITO, Y. (1978). *Acta Cryst.* B**34**, 3149–3156.

WILLIS, B. T. M. (1969). *Acta Cryst.* A**25**, 277–300.

YANG, Y. W. & COPPENS, P. (1974). *Solid State Commun.* **15**, 1555–1559.

ZEMEL, J. N. (1964). *Physics of Semiconductors, Proceedings of the 7th International Conference*, edited by M. HULIN, pp. 1061–1064. New York: Academic Press.

Proper Layer Description and Standard Representation of Inorganic Layered Structure Types*

BY J. LIMA-DE-FARIA

Junta de Investigações Científicas do Ultramar, Alameda D. Afonso Henriques, 41–4°· E., 1000 Lisboa, Portugal

Abstract

A standard representation is proposed for layered structure types (broadly speaking, those that are decomposable in layers), based on a layer description along plane directions. As an example, this standard representation is applied to simple structure types based on cubic closest packing, complemented by an appropriate notation.

Introduction

The aim of this paper is to help establish a certain order and simplicity in the representation of structures, that are decomposable in any kind of layers and not just certain types of layers (*e.g.* Wells, 1975, p. 29). A standard representation is proposed based on the layer description along the most suitable plane directions, and which is inspired by the condensed-model technique (Lima-de-Faria, 1965a). This standard representation has been applied to many close-packed structure types; however, only a group of structure types of simple binary compounds, based on cubic closest packing, will be presented here.

Notation

For a more complete description of the structures we need to include, not only the type of packing layers and their stacking, but also the kind of configuration of the packing atoms in minor proportion and that of the interstitial atoms, *i.e.* their distribution patterns and the way these distribution patterns are superposed within the structures.

The notation used here for the distribution patterns of either packing or interstitial atoms, and their sequences, is an extension of the symbology already used for the description of the layers and their stackings in the general table of inorganic structure types (Lima-de-Faria & Figueiredo, 1976).

The distribution patterns are symbolized by a capital letter indicating the shape of the plane unit cell of their patterns, using T for hexagonal (triangular net), Q for square (quadrangular net), and R for rectangular or oblique shape, and an upper symbol indicating the occupancy of the atoms in the possible sites within this unit cell. For instance Q^{5^2} means a distribution pattern of the type Q with a proportion of occupancy of $\frac{2}{5}$. In the particular cases of proportions of occupancy of $\frac{1}{2}, \frac{1}{3}, \frac{1}{4}, \ldots$ the number one is omitted, for reasons of simplicity, and Q^2 corresponds to a proportion $\frac{1}{2}$; Q^0 corresponds to zero occupancy. In the case of layers with mixed composition the distribution pattern normally refers to the atoms in smaller proportion in the layer, because it generally leads to the simplest description.

The sequence of the distribution pattern either of the packing atoms in minor proportion or of interstitial atoms is indicated by a superscript near the symbol of the distribution pattern, which represents the translation and/or the rotation of the distribution pattern necessary to reproduce its successive positions within